Optim Eng (2006) 7: 173–199
DOI 10.1007/s11081-006-6838-0

Interface cracks in composite orthotropic materials and their delamination via global shape optimization

Victor A. Kovtunenko

Received: 26 April 2004 / Revised: 9 March 2005

Abstract Based on the linear theory of elasticity a model describing two, in-plane deformation identical, homogeneous orthotropic materials coupled at an interface with the angle of 2β between their vertical planes of elastic symmetry and with a crack at the interface is studied. The model under consideration is spatial, and it does not split into independent isotropic/orthotropic in-plane and anti-plane models, which are treated here as the limit case of $\beta = 0/\pm\frac{\pi}{2}$, respectively. The well-posedness of mathematical formulation of the problem is provided by variational methods. Applying a global optimization for the total potential energy with respect to one shape parameter of the crack length, a model for the quasi-static delamination is proposed and compared with the Griffith fracture criterion . Numerical experiments for the composite material with a plane interface crack of the fracture mode-1, mode-2, and mode-3 are presented and analyzed with respect to the half-angle β of coupling and length of the crack.

Keywords Composite material · Interface crack · Crack propagation · Delamination · Shape optimization · Variational methods · Numerical optimization

1. Introduction

Problems with cracks arise from applications in fracture mechanics, and they are of a great importance for structure design in engineering sciences. A complete mathematical formulation of the crack problems can be given in framework of the 3-dimensional theory of elasticity (Morozov, 1984). Nevertheless, a constructive representation of the singularities appearing due to the presence of a crack in a domain, as a rule, is not available in an analytic way. The standard approach to simplify the complete elasticity model consists in splitting of the problem into 2-dimensional in-plane and anti-plane models, which are mainly treated in the

V. A. Kovtunenko
Lavrent'ev Institute of Hydrodynamics, 630090 Novosibirsk, Russia; Institute for Mathematics, University of Graz, 8010 Graz, Austria
e-mail: kovtunenko@hydro.nsc.ru

literature on fracture. The corresponding singularities can be analyzed in an analytic way, but they lose an important information on the spatial state of a physical system. These facts motivated us to study an interim between 2- and 3-, the so-called 2.5-dimensional model. The model is spatial while accounting all 3 components of the displacement vector, but it is formulated in a 2-dimensional domain.

For construction of the 2.5-dimensional model we consider a homogeneous orthotropic material with the vertical plane of elastic symmetry rotated with an angle of β to a reference coordinate system (x_1, x_2, x_3). As the specific case we study a semi-isotropic material, which is fibred along one selected direction of the angle of β with x_3, and it is isotropic in all orthogonal to it cross-sections. Then the assumption of plain deformation is applied at $x_3 = const$. As a result of the rotation we arrive at a spatial model. Next we couple two pieces of such material at the plane interface $x_2 = 0$ with the corresponding angles of $\beta/-\beta$ in upper/ lower half-spaces. Finally, a crack is assumed to be situated at the interface.

In our numerical experiments we observed spatial effects: mixing of crack modes (mode-1 with mode-3) under pure mode-1 as well as mode-3 loading, and mutual inter-penetration between opposite crack surfaces occurring under pure mode-3 loading. Let us emphasize that these effects would be impossible for the 2-dimensional in-plane/ anti-plane model.

For plane models the general approach to analysis of the singularities appearing due to the presence of a crack at an interface between two anisotropic half-planes was described in Ting (1986), Suo (1990), Ni and Nemat-Nasser (1991). The elastic problem for determination of the corresponding singular solutions can be reduced with the help of partial Fourier transformation to a matrix eigenvalue problem by means of the Stroh formalism. An analytic realization of such complicated technique was available for particular cases only. The analytical solutions obtained in Ting (1986), Suo (1990), Ni and Nemat-Nasser (1991) require suitable orientation of the axes of material symmetry to ensure decoupling of the anti-plane fracture mode from the in-plane ones. Alternatively, in Nazarov (1998) (with no assumption of symmetry) there was considered an eigenvalue problem for power solutions (singular solutions of the specific form), which was treated as a self-adjoint system to derive the order of singularity and to define its eigenvectors in a formal way again.

The principal question for fracture mechanics and structure design is to describe the stability properties of a solid having a crack and to predict its growth. By the Griffith fracture hypothesis the propagation of a crack is determined by an energy release rate G_C at the crack tip, which can not exceed a given physical parameter $\gamma > 0$ (see Cherepanov (1979) and Rice (1978)). Namely, the crack does not grow when $G_C < \gamma$, and it starts to propagate by attaining γ:

Griffith criterion: $G_C = \gamma$

There have been a large number of papers concerning the investigation of quasi-static growth of a crack in elastic media (see Morozov (1984), Bach et al. (2000), Bourdin et al. (2000), Kovtunenko (2003, 2004) etc). Various approaches utilizing stress intensity factors for description of the crack propagation were applied in Friedman and Liu (1996), Leblond (1999), Friedman et al. (2000), Argatov et al. (2003). Respective fracture criterions are based on stress characteristics of the crack. Alternatively, energetic fracture criterions involve the consideration of surface energy distributed at a crack. Suggesting a non-constant function for the density of surface energy leads to a refinement of the Griffith fracture hypothesis (e.g. Barenblatt, Dagdale criterions), which can be treated within an optimization approach, see Kovtunenko (2005).

On the other hand, the known Griffith formula, in particular, allows to argue $-G_C$ as a shape derivative $P'(l)$ of the potential energy functional $P(l)$ with respect to variation of the crack length l at the crack tip. Recently in Khludnev and Sokolowski (1999) and Khludnev and Kovtunenko (2000), methods of the shape sensitivity analysis were adopted to a wide class of crack problems with non-penetration conditions. This fact provides us with a general formula for the shape derivative of energy functionals in direction of a chosen velocity field, which includes the Griffith formula as the specific case. Thus, the Griffith fracture criterion possesses the form:

Local minimum: $$\gamma + P'(l) = 0$$

It implies the necessary condition of local minimum (if it exists) with respect to l for the function of total potential energy $\gamma l + P(l)$, where the term γl means the surface energy distributed uniformly at the crack of length l. In a natural way the above local optimality criterion admits a generalization to the global minimization problem over all admissible l:

Global minimum: $$\gamma l + P(l) \to \inf_l$$

Mathematical properties of the shape optimization problem for non-parameterized cracks were analyzed in Francfort and Marigo (1998) and Dal Maso and Toader (2002), and for close time-evolution processes in (Mielke et al., 2002). This is trivial to note that both local and global minima criteria are equivalent for strictly convex functionals P, and they can distinguish them-self for non-convex P. The former case is known as a stable crack propagation (progressive), the latter case of unstable (or brutal) crack growth is most interesting. It was noticed in (Francfort and Marigo, 1998) that for the brutal growth the Griffith fracture law (as local criterion) predicts the critical loading for initiation of the crack propagation larger than one needs using the global minimum criterion. This fact is observed in our numerical tests, too. From the global optimization we obtain not only continuous solutions for the stable crack propagation, but also solutions with jumps and discontinuous velocities of the propagation.

For the numerical calculation of stable as well as unstable paths of the solution we apply a path-following type method allowing jumps. This reminds the results of a one-parametric nonlinear optimization which are based on generalized critical points. Classification and analysis of the singularities of these points was proposed in Guddat and Nowack (1991), and jumps in the set of local minimizers were stressed in Jongen and Stein (1997). For a non-generic problem of the unilateral contact in solid mechanics, stability questions of the solution along the path were examined in Rochde and Stavroulakis (1997).

In the present work we apply the shape optimization approach related to the Griffith fracture law. This problem is solved numerically to describe the delamination of a composite anisotropic solid with an interface crack under the quasi-static linear loading. Note that the delamination process suggests a predefined path (along the interface) of the crack propagation. For bonded isotropic solids the suggestion of straight crack path is not true for mode-2 cracks. In contrast, the inter-laminar fracture of fibred materials under mode-2 loading was confirmed experimentally (König et al., 1997). Hence the hypothesis of delamination is suitable for the suggested model when it describes an inter-laminar crack.

2. Modelling of a composite material with an interface crack

In the first part we formulate a model of composite with crack in dependence of the half-angle β of coupling. We deduce the corresponding representation of elasticity coefficients, constitutive and equilibrium laws. The specific case of material parameters for a semi-isotropic fibred material is described in Section 2.4. Following Sections 2.5 and 2.6 present the plane isotropic and orthotropic models as the limit case of coupling when $\beta = 0$ and $\beta = \pm\pi/2$, respectively.

2.1. Homogeneous orthotropic material in (x'_1, x'_2, x'_3)-axes.

For a displacement vector $u' = (u'_1, u'_2, u'_3)^\top$ given in the Descartes coordinates (x'_1, x'_2, x'_3) we suppose the linear Cauchy law:

$$\varepsilon'_{ij}(u') = 0.5(u'_{i,j} + u'_{j,i}), \quad i, j = 1, 2, 3 \tag{1}$$

Considering the homogeneous orthotropic material whose planes of elastic symmetry correspond to the x'_1, x'_2, x'_3-axes, components of the symmetric (3×3)-tensors of strain $\varepsilon' = \{\varepsilon'_{ij}\}$ and stress $\sigma' = \{\sigma'_{ij}\}$ are connected with the help of a symmetric (6×6)-matrix as follows (Lekhnitskii, 1963):

$$\begin{bmatrix} \sigma'_{11} \\ \sigma'_{22} \\ \sigma'_{33} \\ \sigma'_{12} \\ \sigma'_{23} \\ \sigma'_{13} \end{bmatrix} = \begin{bmatrix} C'_{11} & C'_{12} & C'_{13} & 0 & 0 & 0 \\ C'_{12} & C'_{22} & C'_{23} & 0 & 0 & 0 \\ C'_{13} & C'_{23} & C'_{33} & 0 & 0 & 0 \\ 0 & 0 & 0 & 2C'_{44} & 0 & 0 \\ 0 & 0 & 0 & 0 & 2C'_{55} & 0 \\ 0 & 0 & 0 & 0 & 0 & 2C'_{66} \end{bmatrix} \begin{bmatrix} \varepsilon'_{11} \\ \varepsilon'_{22} \\ \varepsilon'_{33} \\ \varepsilon'_{12} \\ \varepsilon'_{23} \\ \varepsilon'_{13} \end{bmatrix} \tag{2}$$

The elasticity coefficients can be expressed by the relations:

$$\begin{aligned} &C'_{11} = \theta\left(\frac{1}{E_2} - \frac{\nu_{32}^2}{E_3}\right), \quad C'_{12} = \theta\left(\frac{\nu_{21}}{E_2} + \frac{\nu_{31}\nu_{32}}{E_3}\right), \\ &C'_{13} = \theta\left(\frac{\nu_{31} + \nu_{21}\nu_{32}}{E_2}\right), \quad C'_{22} = \theta\left(\frac{1}{E_1} - \frac{\nu_{31}^2}{E_3}\right), \\ &C'_{23} = \theta\left(\frac{\nu_{32}}{E_1} + \frac{\nu_{21}\nu_{31}}{E_2}\right), \quad C'_{33} = \theta\frac{E_3}{E_2}\left(\frac{1}{E_1} - \frac{\nu_{21}^2}{E_2}\right), \\ &C'_{44} = G_{21}, \quad C'_{55} = G_{32}, \quad C'_{66} = G_{31} \end{aligned} \tag{3}$$

where

$$\frac{1}{\theta} = \left(\frac{1}{E_2} - \frac{\nu_{32}^2}{E_3}\right)\left(\frac{1}{E_1} - \frac{\nu_{31}^2}{E_3}\right) - \left(\frac{\nu_{21}}{E_2} + \frac{\nu_{31}\nu_{32}}{E_3}\right)^2 \tag{4}$$

with 9 independent material parameters, which are positive:

$$E_1,\ E_2,\ E_3,\ \nu_{21},\ \nu_{32},\ \nu_{31},\ G_{21},\ G_{32},\ G_{31} \tag{5}$$

2.2. Rotation of (x_1', x_2', x_3') to (x_1, x_2, x_3) around the $x_2' = x_2$-axis.

For a displacement vector $u = (u_1, u_2, u_3)^\top$ in the Descartes coordinates (x_1, x_2, x_3), the rotation of (x_1', x_2', x_3') to (x_1, x_2, x_3) around the common $x_2' = x_2$-axis in anti-clockwise direction with the angle of β between x_3' and x_3 is given by the formula:

$$\begin{bmatrix} u_1 \\ u_2 \\ u_3 \end{bmatrix} = R_2(\beta) \begin{bmatrix} u_1' \\ u_2' \\ u_3' \end{bmatrix}, \quad R_2(\beta) = \begin{bmatrix} \cos\beta & 0 & -\sin\beta \\ 0 & 1 & 0 \\ \sin\beta & 0 & \cos\beta \end{bmatrix} \tag{6}$$

The Cauchy law is assumed linear as before:

$$\varepsilon_{ij}(u) = 0.5(u_{i,j} + u_{j,i}), \quad i, j = 1, 2, 3 \tag{7}$$

According to (2) the corresponding symmetric (3×3)-tensors of strain $\varepsilon = \{\varepsilon_{ij}\}$ and stress $\sigma^\beta = \{\sigma_{ij}^\beta\}$ can be connected by a (6×6)-matrix:

$$\begin{bmatrix} \sigma_{11}^\beta \\ \sigma_{22}^\beta \\ \sigma_{33}^\beta \\ \sigma_{12}^\beta \\ \sigma_{23}^\beta \\ \sigma_{13}^\beta \end{bmatrix} = \begin{bmatrix} C_{11}^\beta & C_{12}^\beta & C_{13}^\beta & 0 & 0 & 2C_{16}^\beta \\ C_{12}^\beta & C_{22} & C_{23}^\beta & 0 & 0 & 2C_{26}^\beta \\ C_{13}^\beta & C_{23}^\beta & C_{33}^\beta & 0 & 0 & 2C_{36}^\beta \\ 0 & 0 & 0 & 2C_{44}^\beta & 2C_{45}^\beta & 0 \\ 0 & 0 & 0 & 2C_{45}^\beta & 2C_{55}^\beta & 0 \\ C_{16}^\beta & C_{26}^\beta & C_{36}^\beta & 0 & 0 & 2C_{66}^\beta \end{bmatrix} \begin{bmatrix} \varepsilon_{11} \\ \varepsilon_{22} \\ \varepsilon_{33} \\ \varepsilon_{12} \\ \varepsilon_{23} \\ \varepsilon_{13} \end{bmatrix} \tag{8}$$

with the following 13 coefficients:

$$\begin{aligned}
C_{33}^\beta &= C_{33}' \cos^4\beta + 2(C_{13}' + 2C_{66}') \sin^2\beta \cos^2\beta + C_{11}' \sin^4\beta, \\
C_{11}^\beta &= C_{33}' \sin^4\beta + 2(C_{13}' + 2C_{66}') \sin^2\beta \cos^2\beta + C_{11}' \cos^4\beta, \\
C_{13}^\beta &= C_{13}' + (C_{33}' + C_{11}' - 2C_{13}' - 4C_{66}') \sin^2\beta \cos^2\beta, \\
C_{66}^\beta &= C_{66}' + (C_{33}' + C_{11}' - 2C_{13}' - 4C_{66}') \sin^2\beta \cos^2\beta, \\
C_{36}^\beta &= [C_{11}' \sin^2\beta - C_{33}' \cos^2\beta + (C_{13}' + 2C_{66}')(\cos^2\beta - \sin^2\beta)] \sin\beta \cos\beta, \\
C_{16}^\beta &= [C_{11}' \cos^2\beta - C_{33}' \sin^2\beta - (C_{13}' + 2C_{66}')(\cos^2\beta - \sin^2\beta)] \sin\beta \cos\beta, \\
C_{44}^\beta &= C_{44}' \cos^2\beta + C_{55}' \sin^2\beta, \\
C_{55}^\beta &= C_{44}' \sin^2\beta + C_{55}' \cos^2\beta, \\
C_{45}^\beta &= (C_{44}' - C_{55}') \sin\beta \cos\beta, \\
C_{23}^\beta &= C_{23}' \cos^2\beta + C_{12}' \sin^2\beta, \\
C_{12}^\beta &= C_{23}' \sin^2\beta + C_{12}' \cos^2\beta, \\
C_{26}^\beta &= (C_{12}' - C_{23}') \sin\beta \cos\beta, \\
C_{22} &= C_{22}'
\end{aligned} \tag{9}$$

2.3. Plane deformation model when u does not depend on x_3

If $u(x_1, x_2)$ does not depend on x_3, then $\varepsilon_{33} = 0$ and the strain tensor in (7) takes the particular form:

$$\begin{aligned}
&\varepsilon_{11}(u) = u_{1,1}, \qquad \varepsilon_{22}(u) = u_{2,2},\\
&\varepsilon_{12}(u) = 0.5(u_{1,2} + u_{2,1}),\\
&\varepsilon_{13}(u) = 0.5u_{3,1}, \quad \varepsilon_{23}(u) = 0.5u_{3,2}
\end{aligned} \tag{10}$$

Components of the stress tensor in (8) admits the representation:

$$\begin{aligned}
\sigma^{\beta}_{11}(u) &= C^{\beta}_{11}u_{1,1} + C^{\beta}_{12}u_{2,2} + C^{\beta}_{16}u_{3,1},\\
\sigma^{\beta}_{22}(u) &= C^{\beta}_{12}u_{1,1} + C_{22}u_{2,2} + C^{\beta}_{26}u_{3,1},\\
\sigma^{\beta}_{12}(u) &= C^{\beta}_{44}(u_{1,2} + u_{2,1}) + C^{\beta}_{45}u_{3,2},\\
\sigma^{\beta}_{23}(u) &= C^{\beta}_{45}(u_{1,2} + u_{2,1}) + C^{\beta}_{55}u_{3,2},\\
\sigma^{\beta}_{13}(u) &= C^{\beta}_{16}u_{1,1} + C^{\beta}_{26}u_{2,2} + C^{\beta}_{66}u_{3,1}
\end{aligned} \tag{11}$$

with 9 coefficients from list (9):

$$C^{\beta}_{11},\ C^{\beta}_{66},\ C^{\beta}_{16},\ C^{\beta}_{44},\ C^{\beta}_{55},\ C^{\beta}_{45},\ C^{\beta}_{12},\ C^{\beta}_{26},\ C_{22} \tag{12}$$

For the formulation of an equilibrium problem following later, the vector of $\operatorname{div}\sigma^{\beta}$ can be expressed from (11) as:

$$\begin{aligned}
\sigma^{\beta}_{1j,j}(u) &= C^{\beta}_{11}u_{1,11} + C^{\beta}_{44}u_{1,22} + \big(C^{\beta}_{12} + C^{\beta}_{44}\big)u_{2,12} + C^{\beta}_{16}u_{3,11} + C^{\beta}_{45}u_{3,22},\\
\sigma^{\beta}_{2j,j}(u) &= \big(C^{\beta}_{12} + C^{\beta}_{44}\big)u_{1,12} + C^{\beta}_{44}u_{2,11} + C_{22}u_{2,22} + \big(C^{\beta}_{45} + C^{\beta}_{26}\big)u_{3,12},\\
\sigma^{\beta}_{3j,j}(u) &= C^{\beta}_{16}u_{1,11} + C^{\beta}_{45}u_{1,22} + \big(C^{\beta}_{45} + C^{\beta}_{26}\big)u_{2,12} + C^{\beta}_{66}u_{3,11} + C^{\beta}_{55}u_{3,22}
\end{aligned} \tag{13}$$

where the summation convention for the repeated indices $i,\ j = 1, 2, 3$ is used.

2.4. Semi-isotropic material fibred along the x_3'-axis

As the specific case we consider the material being isotropic in every plane $x_3' = const$ and fibred along the x_3'-axis. This assumption implies the identities:

$$\begin{aligned}
&E_1 = E_2 = E, \quad \nu_{21} = \nu, \quad G_{21} = \frac{E}{2(1+\nu)},\\
&\nu_{31} = \nu_{32} = \nu_3, \quad G_{31} = G_{32} = G_3
\end{aligned} \tag{14}$$

which reduces list (5) of the independent material parameters to the following 5:

$$E,\ E_3,\ \nu,\ \nu_3,\ G_3 \tag{15}$$

Instead of (4) we denote:

$$\frac{1}{\kappa} = \frac{1-\nu}{E} - \frac{2\nu_3^2}{E_3} = \left(\frac{1}{E} - \frac{\nu_3^2}{E_3}\right) - \left(\frac{\nu}{E} + \frac{\nu_3^2}{E_3}\right) \tag{16}$$

and rewrite coefficients in (3) as:

$$\begin{aligned} &C'_{11} = C'_{22} = \kappa\frac{E}{1+\nu}\left(\frac{1}{E} - \frac{\nu_3^2}{E_3}\right), \quad C'_{12} = \kappa\frac{E}{1+\nu}\left(\frac{\nu}{E} + \frac{\nu_3^2}{E_3}\right), \\ &C'_{13} = C'_{23} = \kappa\nu_3, \quad C'_{33} = \kappa\frac{E_3}{E}(1-\nu), \\ &C'_{44} = \frac{E}{2(1+\nu)}, \quad C'_{55} = C'_{66} = G_3 \end{aligned} \tag{17}$$

In this case, elasticity coefficients fulfill the relations:

$$C'_{12} + 2C'_{44} = C'_{11} = C'_{22}, \quad C'_{12} + C'_{44} = 0.5\,\kappa \tag{18}$$

The angle $\beta \in [-\pi/2, \pi/2]$ determines the corresponding plane deformation model (8)–(9). Next we consider the limit cases of coupling when $\beta = 0$ and $\beta = \pi/2$.

2.5. Plane isotropic model as $\beta = 0$

As $\beta = 0$ the coefficients in (9) are as follows:

$$\begin{aligned} &C^0_{11} = C_{22} = \kappa\frac{E}{1+\nu}\left(\frac{1}{E} - \frac{\nu_3^2}{E_3}\right), \quad C^0_{12} = \kappa\frac{E}{1+\nu}\left(\frac{\nu}{E} + \frac{\nu_3^2}{E_3}\right), \\ &C^0_{44} = \frac{E}{2(1+\nu)}, \quad C^0_{55} = C^0_{66} = G_3, \quad C^0_{16} = C^0_{26} = C^0_{45} = 0 \end{aligned} \tag{19}$$

The stress tensor from (11) is split into components for $(u_1, u_2)^\top$:

$$\begin{aligned} &\sigma^0_{11}(u) = C^0_{11}u_{1,1} + C^0_{12}u_{2,2}, \\ &\sigma^0_{22}(u) = C^0_{12}u_{1,1} + C_{22}u_{2,2}, \\ &\sigma^0_{12}(u) = C^0_{44}(u_{1,2} + u_{2,1}) \end{aligned} \tag{20}$$

and independently for u_3:

$$\sigma^0_{23}(u) = C^0_{55}u_{3,2}, \quad \sigma^0_{13}(u) = C^0_{66}u_{3,1} \tag{21}$$

Let us introduce the notation:

$$\mu = \frac{E}{2(1+\nu)}, \quad \lambda = \kappa\frac{E}{1+\nu}\left(\frac{\nu}{E} + \frac{\nu_3^2}{E_3}\right) \tag{22}$$

In view of (18) the next relations between elasticity coefficient are fulfilled:

$$\begin{aligned} &C^0_{11} = C_{22} = C^0_{12} + 2C^0_{44} = \lambda + 2\,\mu, \\ &C^0_{12} + C^0_{44} = \lambda + \mu = 0.5\,\kappa \end{aligned} \tag{23}$$

As a result we arrive at a 2-dimensional Lamé/ Laplace operator for the in-plane/ anti-plane isotropic problem:

$$\begin{aligned}
&\sigma^0_{1j,j}(u) = \mu\Delta u_1 + (\lambda+\mu)(\operatorname{div} u)_{,1},\\
&\sigma^0_{2j,j}(u) = \mu\Delta u_2 + (\lambda+\mu)(\operatorname{div} u)_{,2},\\
&\sigma^0_{3j,j}(u) = G_3\Delta u_3
\end{aligned} \tag{24}$$

depending on the Lamé parameters λ, μ given in (22) and the material parameter G_3, where $\operatorname{div} u = u_{1,1} + u_{2,2}$ and $\Delta u_i = u_{i,11} + u_{i,22}$, $i = 1, 2, 3$.

2.6. Plane orthotropic model as $\beta = \pi/2$

As $\beta = \pi/2$ the coefficients in (9) read:

$$\begin{aligned}
&C^{\pi/2}_{11} = \kappa\frac{E_3}{E}(1-\nu), \quad C_{22} = \kappa\frac{E}{1+\nu}\left(\frac{1}{E} - \frac{\nu_3^2}{E_3}\right), \quad C^{\pi/2}_{12} = \kappa\nu_3,\\
&C^{\pi/2}_{55} = \frac{E}{2(1+\nu)}, \quad C^{\pi/2}_{44} = C^{\pi/2}_{66} = G_3, \quad C^{\pi/2}_{16} = C^{\pi/2}_{26} = C^{\pi/2}_{45} = 0
\end{aligned} \tag{25}$$

In this case, the stress tensor from (11) is split similarly to (20) and (21), too, and calculations lead to the following operator for the in-plane/anti-plane orthotropic problem:

$$\begin{aligned}
&\sigma^{\pi/2}_{1j,j}(u) = \kappa\frac{E_3}{E}(1-\nu)u_{1,11} + G_3u_{1,22} + (\kappa\nu_3 + G_3)u_{2,12},\\
&\sigma^{\pi/2}_{2j,j}(u) = (\kappa\nu_3 + G_3)u_{1,12} + G_3u_{2,11} + (2\mu+\lambda)u_{2,22},\\
&\sigma^{\pi/2}_{3j,j}(u) = G_3u_{3,11} + \mu u_{3,22}
\end{aligned} \tag{26}$$

All above formulas keep itself by inverting $\beta = \pi/2$ to $\beta = -\pi/2$. Thus, we can conclude that the spatial model (8)–(9) is interim between the plane isotropic model as $\beta = 0$ and the plane orthotropic model as $\beta = \pm\pi/2$.

2.7. Composite material with an interface crack

We compose the same material with parameters from (5) and coefficients from (3), (4) given with respect to (x_1', x_2', x_3')-axes: with the angle of $\beta \in [-\pi/2, \pi/2]$ between the axis x_3' and x_3 in the "upper" half-space $\mathbb{R}^3_+ = \{x_1, x_2 = x_2' \geq 0, x_3\}$, and with the angle of $-\beta$ in the "lower" half-space $\mathbb{R}^3_- = \{x_1, x_2 = x_2' \leq 0, x_3\}$, as it is illustrated in Figure 1. In $\mathbb{R}^3_-$ all previous formulas are valid when β is replaced with $-\beta$. The materials are assumed to be joined on the interface $x_2 = 0$. In the composite material consider the displacement, stress:

$$u = \begin{cases} u^+ & \text{in } \mathbb{R}^3_+,\\ u^- & \text{in } \mathbb{R}^3_-, \end{cases} \quad \sigma(u) = \begin{cases} \sigma^{\beta}(u^+) & \text{in } \mathbb{R}^3_+\\ \sigma^{-\beta}(u^-) & \text{in } \mathbb{R}^3_- \end{cases} \tag{27}$$

and the strain from (7). We suppose that the plane deformation of the composite material is realized as before, i.e $u(x_1, x_2)$ does not depend on x_3.

Let a crack be posed at the interface $x_2 = 0$. To determine singular solutions admissible here one has to look for the homogeneous boundary-value problem of linear elasticity in

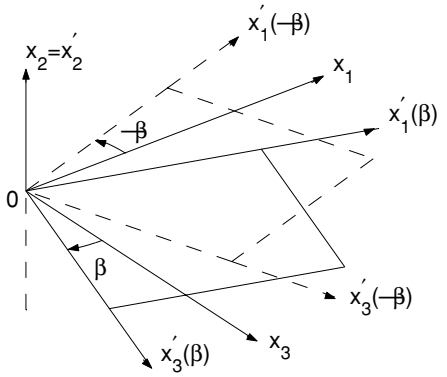

Fig. 1 Composite of materials in $\mathbb{R}^3_\pm$

the plane $\mathbb{R}^2 = \mathbb{R}^2_+ \cup \mathbb{R}^2_-$, where $\mathbb{R}^2_\pm = \{x_1, \pm x_2 \geq 0\}$, with the crack. Due to the identities fulfilled between the elasticity coefficients:

$$\begin{aligned} &C^{\beta}_{11} = C^{-\beta}_{11},\ C^{\beta}_{12} = C^{-\beta}_{12},\ C^{\beta}_{44} = C^{-\beta}_{44},\ C^{\beta}_{55} = C^{-\beta}_{55},\ C^{\beta}_{66} = C^{-\beta}_{66}, \\ &C^{\beta}_{16} = -C^{-\beta}_{16},\ C^{\beta}_{26} = -C^{-\beta}_{26},\ C^{\beta}_{45} = -C^{-\beta}_{45} \end{aligned} \tag{28}$$

we arrive at the equivalent singular problem in the half-plane:

$$\begin{aligned} &-\operatorname{div} \sigma^{\beta}(u^+) = 0 \quad \text{in } \mathbb{R}^2_+ \setminus \{x_2 = 0\}, \\ &\sigma^{\beta}_{12}(u^+) = \sigma^{\beta}_{22}(u^+) = \sigma^{\beta}_{23}(u^+) = 0 \quad \text{on } \{x_2 = 0, x_1 < 0\}, \\ &u^+_3 = \sigma^{\beta}_{23}(u^+) = 0 \quad \text{on } \{x_2 = 0, x_1 \geq 0\} \end{aligned} \tag{29}$$

for the following function

$$(u_1, u_2, u_3)^\top = \begin{cases} (u^+_1, u^+_2, u^+_3)^\top & \text{in } \mathbb{R}^2_+ \\ (u^+_1, u^+_2, -u^+_3)^\top & \text{in } \mathbb{R}^2_- \end{cases} \tag{30}$$

3. Problem with an interface crack in the composite material and its delamination

Using representations from Section 2 of elasticity coefficients, constitutive and equilibrium laws, in the second part we get boundary-value and variational formulations of an equilibrium problem for the composite with crack, and we describe the quasi-static process of its delamination via global shape optimization approach. Their features by numerical realization will be discussed in Section 4.

3.1. Equilibrium problem of the solid with crack

Let us consider the composite of two elastic orthotropic solids joined along the plane $x_2 = 0$, which was described in Section 2. We assume that, in all cross-sections $x_3 = const$, it occupies a domain $\Omega \subset \mathbb{R}^2$ consisted of two sub-domains $\Omega^+ \subset \mathbb{R}^2_+$ and $\Omega^- \subset \mathbb{R}^2_-$ with

the interface Σ on $x_2 = 0$, i.e. $\Omega = \Omega^+ \cup \Omega^- \cup \Sigma$. Let Ω be bounded by the Lipschitz boundary $\partial\Omega = \Gamma_N \cup \Gamma_D$, where $\Gamma_D \neq \emptyset$, with an outward normal vector $n = (n_1, n_2)^\top$.

We suppose that a crack Γ_C is situated at the interface Σ, and we consider a domain with crack $\Omega_C = \Omega \setminus \overline{\Gamma}_C$. Its boundary $\partial\Omega_C$ includes Γ_N, Γ_D, and the crack surfaces $\Gamma_C^\pm$. Here $\Gamma_C^+ \subset \Sigma^+$ and $\Gamma_C^- \subset \Sigma^-$ are defined as a limit of points $x \in \Omega^+$ and $x \in \Omega^-$ going to Σ, respectively. We describe the interface crack problem by the following linear relations:

$$
\begin{aligned}
&-\operatorname{div}\sigma(u) = f \quad \text{in } \Omega_C,\\
&\sigma_{12}(u) = \sigma_{22}(u) = \sigma_{23}(u) = 0 \quad \text{on } \Gamma_C^\pm,\\
&[\![u]\!] = 0, \quad [\![\sigma_{12}(u)]\!] = [\![\sigma_{22}(u)]\!] = [\![\sigma_{23}(u)]\!] = 0 \quad \text{on } \Sigma \setminus \Gamma_C,\\
&\sigma(u)\cdot n = g \quad \text{on } \Gamma_N,\\
&u = 0 \quad \text{on } \Gamma_D
\end{aligned}
\tag{31}
$$

where $[\![u]\!] = u|_{\Sigma^+} - u|_{\Sigma^-}$ and $[\![\sigma(u)]\!] = \sigma(u)|_{\Sigma^+} - \sigma(u)|_{\Sigma^-}$ imply the jump across the interface, and notation (27) is utilized. Given $f = (f_1, f_2, f_3)^\top$ and $g = (g_1, g_2, g_3)^\top$ present a volume load and a boundary traction, respectively.

3.2. Variational formulation of the interface crack problem

Let us introduce the Sobolev space of admissible displacements:

$$
H(\Omega_C) = \{u \in H^1(\Omega_C)^3 : \quad u = 0 \quad \text{on } \Gamma_D\} \tag{32}
$$

For $f \in L^2(\Omega_C)^3$ and $g \in L^2(\Gamma_N)^3$, the weak solution $u \in H(\Omega_C)$ to (31) is defined by the variational equation:

$$
\int_{\Omega_C} \sigma_{ij}(u)\varepsilon_{ij}(v)\,dx = \int_{\Omega_C} f v\,dx + \int_{\Gamma_N} g v\,ds \quad \text{for all } v \in H(\Omega_C) \tag{33}
$$

For a unique solvability of (33), the uniform positiveness of the quadratic term is required:

$$
c_0(\beta) > 0 : \quad \int_{\Omega_C} \sigma_{ij}(u)\varepsilon_{ij}(u)\,dx \geq c_0(\beta)\|u\|^2_{H(\Omega_C)} \quad \text{for all } u \in H(\Omega_C) \tag{34}
$$

If the (5×5)-matrix in (11) was positive defined for some β this would lead to the estimate:

$$
\lambda_{\min}(\beta) > 0 : \quad \int_{\Omega_C} \sigma_{ij}(u)\varepsilon_{ij}(u)\,dx \geq \lambda_{\min}(\beta) \int_{\Omega_C} \varepsilon_{ij}(u)\varepsilon_{ij}(u)\,dx \tag{35}
$$

with the minimal eigenvalue $\lambda_{\min}(\beta)$ of the matrix. In this case, the Korn-type estimation of (35) from below follows (34).

3.3. Potential energy and its shape derivative

We introduce a quadratic functional of the potential energy:

$$
\Pi(v; \Gamma_C) = \frac{1}{2}\int_{\Omega_C} \sigma_{ij}(v)\varepsilon_{ij}(v)\,dx - \int_{\Omega_C} f v\,dx - \int_{\Gamma_N} g v\,ds \tag{36}
$$

Variational problem (33) is equivalent to the minimization of Π over all $v \in H(\Omega_C)$. Hence the reduced functional is defined in dependence of the crack:

$$P(\Gamma_C) := \Pi(u; \Gamma_C) = \min_{v \in H(\Omega_C)} \Pi(v; \Gamma_C) \tag{37}$$

For some fixed parameter $t \geq 0$, we consider a shape perturbation of the crack by means of the coordinate transformation $y = \Phi(s, x)$ in $\mathbb{R}^2$ for Φ such that:

$$\frac{d}{ds}\Phi(s, \cdot) = V(s, \Phi(s, \cdot)) \quad \text{for } s \neq t, \quad \Phi(t, \cdot) = x \tag{38}$$

with the given velocity field $V(t, x) = (V_1, V_2)^\top \in C([0, \infty); Lip(\mathbb{R}^2))^2$. If V is supported strictly inside Ω, then the corresponding shape derivative of (37) in direction V can be found by formula (Kovtunenko, 2003):

$$\begin{aligned} P'_V(\Gamma_C) &:= \lim_{s \to t} (s - t)^{-1}(P(\Gamma_C \circ \Phi(s)) - P(\Gamma_C)) \\ &= \int_{\Omega_C} \sigma_{ij}(u)\left(\frac{1}{2}\mathrm{div}\, V \varepsilon_{ij}(u) - E_{ij}(\nabla V; u)\right) dx - \int_{\Omega_C} \mathrm{div}\,(V f_i) u_i \, dx \end{aligned} \tag{39}$$

where u is a solution to (33), and the symmetric (3×3)-tensor E denotes generalized strains:

$$E_{ij}(\nabla V; u) = 0.5\,(u_{i,\alpha} V_{\alpha,j} + u_{j,\alpha} V_{\alpha,i}), \quad i, j = 1, 2, 3 \tag{40}$$

The summation convention over repeated indices $\alpha = 1, 2$ is used here.

For the rectilinear crack Γ_C located onto $x_2 = 0$, perturbations along the interface are described by a tangential velocity of the form $V = (\chi, 0)^\top$ with the given first component $\chi(t, x)$. From (39) it follows that:

$$P'_\chi(\Gamma_C) = \int_{\Omega_C} \sigma_{ij}(u)\left(\frac{1}{2}\chi_{,1}\varepsilon_{ij}(u) - E_{ij}(\nabla \chi; u)\right) dx - \int_{\Omega_C} (\chi f_i)_{,1} u_i \, dx \tag{41}$$

and (40) implies:

$$\begin{aligned} &E_{11}(\nabla \chi; u) = \chi_{,1} u_{1,1}, \quad E_{22}(\nabla \chi; u) = \chi_{,2} u_{2,1}, \\ &E_{12}(\nabla \chi; u) = 0.5(\chi_{,2} u_{1,1} + \chi_{,1} u_{2,1}), \\ &E_{23}(\nabla \chi; u) = 0.5\chi_{,2} u_{3,1}, \quad E_{13}(\nabla \chi; u) = 0.5\chi_{,1} u_{3,1} \end{aligned} \tag{42}$$

If χ is supported in a neighborhood B_0 of the crack tip, then $-P'_\chi(\Gamma_C)$, scaled with the value of χ in the vicinity, expresses an energy release rate independently of χ. In fact, let $\chi = 1$ in an arbitrary fixed neighborhood $B \subset B_0$ including the crack tip, with an outward normal $b = (b_1, b_2)^\top$ at the boundary ∂B, and let $f = 0$ in B. Integrating with parts of (41) due to (31) follows an equivalent representation of the derivative as the integral over closed contour (Kovtunenko, 2003):

$$P'_\chi(\Gamma_C) = \int_{\partial B} \sigma_{ij}(u)\left(\frac{1}{2} b_1 \varepsilon_{ij}(u) - E_{ij}(b; u)\right) ds \tag{43}$$

Here b_1 and b_2 replace $\chi_{,1}$ and $\chi_{,2}$ in (42), respectively. For $\beta = 0$ and $u_3 = const$ formula (43) implies the Cherepanov–Rice path-independent integral well known for the plane isotropic model.

3.4. Quasi-static version of the interface crack problem

We suppose that the rectilinear crack Γ_C is given at the interface $\Sigma = \{0 < x_1 < L, x_2 = 0\}$ as the set:

$$\Gamma_C = \{0 < x_1 < l, \quad x_2 = 0\}, \quad 0 < l < L \tag{44}$$

Namely, the left crack-tip $(0, 0)^\top$ is fixed on the boundary $\partial\Omega$, the right tip $(l, 0)^\top$ lives at the interface inside Ω, and the point $(L, 0)^\top$ implies a meeting of the crack with $\partial\Omega$.

In such a way Γ_C can be expressed equivalently by one parameter l of the crack length. Due to (39) we have a function of the potential energy in (37), which is smooth in l:

$$P(l) := P(\Gamma_C) \in C([0, L]), \quad P'(l) := P'_\chi(\Gamma_C) \in C(0, L) \tag{45}$$

The shape derivative can be calculated by formulas (43) or (41) for an arbitrary cut-off function χ supported in a neighborhood B_0 of the crack tip such that $(l, 0)^\top \subset B \subset B_0$ with $\chi = 1$ in B. Note that the minimization in (37) leads to the fact that $P(l)$ is a decreasing function in l, which is uniformly bounded:

$$0 \geq P(\bar{l}) \geq P(l) \geq P(L) \quad \text{for } 0 \leq \bar{l} \leq l \leq L \tag{46}$$

Henceforth, its differentiability implies the property:

$$P'(l) \leq 0 \tag{47}$$

Let $t > 0$ be a parameter of the loading, which is assumed monotonically increasing, namely, linear in (31):

$$f(t) = tf, \quad g(t) = tg \tag{48}$$

In view of the linearity of problem (33) it follows that $u(t) = tu$ is a solution of the quasi-static problem related to (48):

$$\int_{\Omega_C} \sigma_{ij}(u(t))\varepsilon_{ij}(v)\,dx = \int_{\Omega_C} tf v\,dx + \int_{\Gamma_N} tg v\,ds \quad \text{for all } v \in H(\Omega_C) \tag{49}$$

From (49) we arrive finally at the function of the reduced potential energy which is quadratic in t:

$$P(l)(t) = t^2 P(l), \quad P'(l)(t) = t^2 P'(l) \tag{50}$$

3.5. Delamination via one-parametric shape optimization

It was observed in experiments (König et al., 1997) that the fracture of laminar along an interface would be consistent from a physical viewpoint. To describe the delamination between Ω^+ and Ω^- in our model, we fix an initial crack of the length l_0 at $t = 0$, and we look for its quasi-static propagation $l(t) \geq l_0$ with respect to the loading parameter $t > 0$. This formulation implies that the propagation path is predefined a-priori along the interface Σ.

In addition to the potential energy $P(\Gamma_C)$ let us consider the surface energy at the crack surfaces $\Gamma_C^{\pm}$:

$$S(l) := S(\Gamma_C) = \gamma l \tag{51}$$

when the function of energy density is assumed constant. By the principle of virtual work we have to minimize the total potential energy as the sum of potential and surface energies. In this way from (50) and (51) we arrive at the shape optimization problem with respect to the parameter l of crack-length at every "time" t:

$$\gamma l + t^2 P(l) \;\rightarrow\; \inf \quad \text{with respect to } l \in [l_0, L] \quad \text{for } t \geq 0 \tag{52}$$

Due to the linearity of S properties (45) and (46) hold true for $\gamma l + t^2 P(l)$, too. Hence there exists a global minimizer $l(t) \in [l_0, L]$ to (52) such that:

$$\gamma l(t) + t^2 P(l(t)) \leq \gamma l + t^2 P(l) \quad \text{for all } l \in [l_0, L], \quad t \geq 0 \tag{53}$$

Note that $l(t)$ is an increasing function of t:

$$l(t) \geq l(s) \quad \text{for } t > s \tag{54}$$

As $t = 0$ we obtain evidently the initial crack:

$$l(0) = l_0 \tag{55}$$

From (53) it follows directly the inequalities for $t \geq 0$:

$$\gamma l(t) + t^2 P(l(t)) \leq \gamma l + t^2 P(l) \quad \text{for all } l \geq l^-(t) \tag{56}$$

$$\gamma l(t) + t^2 P(l(t)) \leq \gamma l(s) + t^2 P(l(s)) \quad \text{for all } s \leq t \tag{57}$$

where $l^{\pm}(t) = \lim_{s \to t} l(s)$ for $\pm(s - t) > 0$. Relations (54), (55), (56), and (57) form the system of necessary and sufficient conditions for (53), see Francfort and Marigo (1998). In view of the differentiability of P, (56) leads to the necessary condition:

$$\gamma + t^2 P'(l(t)) \geq 0 \tag{58}$$

and the next condition at a jump, which is available by the model, is a consequence of (57):

$$\gamma [l^+(t) - l^-(t)] + t^2 [P(l^+(t)) - P(l^-(t))] = 0 \tag{59}$$

If $l(t)$ was an uniformly continuous function, then the Griffith law of fracture would be satisfied:

$$l(0) = l_0,\ l'(t) \geq 0,\ \gamma + t^2 P'(l(t)) \geq 0,\ l'(t)(\gamma + t^2 P'(l(t))) = 0 \tag{60}$$

Due to (47) from (60) we define a function of the critical loading parameter:

$$G(t, l) := t - \sqrt{\gamma/(-P'(l))}, \quad P'(l) \neq 0 \tag{61}$$

To get a more constructive criterion for the global minimizer to (53), in view of (45) and (58) we introduce the set of critical points:

$$M_t = \left\{ \begin{array}{l} L \\ l_0 \quad \text{if } G(t, l_0) \leq 0 \quad \text{or } P'(l_0) = 0 \\ l:\ G(t, l) = 0 \quad \text{if } l \geq l(s) \text{ for } s \leq t \end{array} \right\} \tag{62}$$

Then (53) is equivalent to:

$$l(0) = l_0, \quad \gamma l(t) + t^2 P(l(t)) = \min_{l \in M_t} \{\gamma l + t^2 P(l)\} \quad \text{for } t > 0 \tag{63}$$

We will discuss the suggested shape optimization problem more detailed on numerical examples following in Section 4.

4. Numerical experiments

The largest third part of the paper deals with a discrete problem, and it provides the theoretical consideration of Sections 2 and 3 with numerical tests, which are discussed. The cases of mode-1, mode-2, and mode-3 loading are treated separately in Section 4.3–4.6, respectively.

4.1. Geometric data for calculations

For numerical experiments we fix the following symmetric geometry of the composed solid with crack presented in Figure 2. Namely, the square domain Ω in $\mathbb{R}^2$ has the boundary:

$$\Gamma_D = \{x_1 = 1, |x_2| \leq 0.5\}, \quad \Gamma_N = \Gamma_{N1}^+ \cup \Gamma_{N1}^- \cup \Gamma_{N2}^+ \cup \Gamma_{N2}^-,$$
$$\Gamma_{N1}^{\pm} = \{x_1 = 0, 0 \leq \pm x_2 \leq 0.5\}, \quad \Gamma_{N2}^{\pm} = \{0 < x_1 < 1, x_2 = \pm 0.5\}$$

We assume that the crack Γ_C of the length $0 < l < L = 1$ lives at the interface $\Sigma = \{0 < x_1 < 1, x_2 = 0\}$ in Ω, and the corresponding faces $\Gamma_C^{\pm}$ of the crack and $\Sigma^{\pm}$ of the interface are defined in $\Omega^{\pm} = \Omega \cap \mathbb{R}^2_{\pm}$, respectively. Then the plane domain with crack $\Omega_C = \Omega \setminus \overline{\Gamma}_C$ is bounded by Γ_D, Γ_N, and $\Gamma_C^{\pm}$.

Fig. 2 Geometry of domain Ω_C

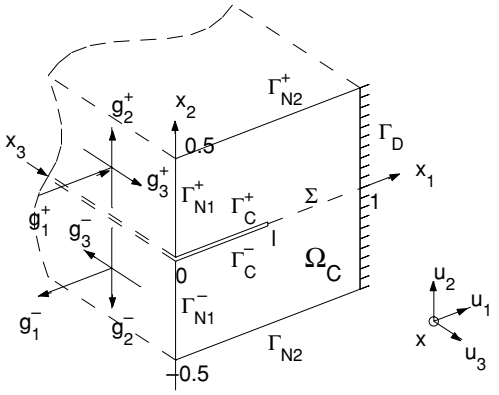

The equilibrium problem in (31) is detailed with the clamping condition at Γ_D, stress-free boundaries $\Gamma_{N2}^{\pm}$ and $\Gamma_C^{\pm}$, volume load $f = 0$, and the traction stated at $\Gamma_{N1}^{\pm}$, as follows:

$$\begin{aligned}
&-\mathrm{div}\,\sigma(u) = 0 \quad \text{in } \Omega_C,\\
&\sigma_{12}(u) = \sigma_{22}(u) = \sigma_{23}(u) = 0 \quad \text{on } \Gamma_C^{\pm} \cup \Gamma_{N2}^{\pm},\\
&-\sigma_{11}(u) = g_1^{\pm},\ -\sigma_{12}(u) = g_2^{\pm},\ -\sigma_{13}(u) = g_3^{\pm} \quad \text{on } \Gamma_{N1}^{\pm},\\
&u_1 = u_2 = u_3 = 0 \quad \text{on } \Gamma_D
\end{aligned} \tag{64}$$

The anti-symmetric loading is applied which utilizes fracture mode-1, mode-2, mode-3 states illustrated in Figure 2. These three cases will be treated separately in Sections 4.3–4.6, respectively.

For material parameters (14) we use the following values (König et al., 1997):

$$\begin{aligned}
&E = 10160(mPa),\ E_3 = 139400(mPa),\ G_3 = 4600(mPa),\\
&\nu = 0.436,\ \nu_3 = 0.3
\end{aligned} \tag{65}$$

corresponding to the semi-isotropic fibred material of Section 2.4. Then the interface crack problem formulated in Section 3.2 is well posed. Indeed, the corresponding minimal eigenvalues $\lambda_{\min}(\beta)$ are found positive, and they have approximately the constant value $\lambda_{\min} \approx 3537.6$ for all $\beta \in [-\pi/2, \pi/2]$. Thus (34) holds true in this case.

The half-angle β of coupling is taken at five equal-spaced points in the interval $[0, \pi/2]$. It presents the plane isotropic model of Section 2.5 as $\beta = 0$, plane orthotropic model of Section 2.6 as $\beta = \pi/2$, and interim spatial models when $\beta = \pi/8$, $\beta = \pi/4$, and $\beta = 3\pi/8$.

Now let us consider the remaining interval $(-\pi/2, 0)$ of admissible β. Let $u = (u_1, u_2, u_3)^\top$ be a solution to (64) for some fixed $\beta \in [0, \pi/2]$. Due to the symmetry properties of data and (28), from (11) we can deduce that $(u_1, u_2, -u_3)^\top$ satisfies (64) with $-\beta$ for $g_1^+ = -g_1^-$, $g_2^+ = -g_2^-$, $g_3^{\pm} = 0$, and $(-u_1, -u_2, u_3)^\top$ fulfils (64) for $g_1^{\pm} = g_2^{\pm} = 0$, $g_3^+ = -g_3^-$. The value of potential energy remains the same by inverting β to $-\beta$. In such a way we can extend solutions of (64) obtained for $\beta \in [0, \pi/2]$ onto the interval of $\beta \in [-\pi/2, 0)$.

For mode-3 loading we observe that the displacement u_2 (i.e. in direction across the crack) changes its sign by inverting β to $-\beta$. Therefore, the jump $[\![u_2]\!] = u_2|_{\Gamma_C^+} - u_2|_{\Gamma_C^-}$ across the crack Γ_C is negative for $-\beta$ when it is positive for β, and visa versa. The negative

jump $[\![u_2]\!] < 0$ means an inter-penetration between the crack surfaces Γ_C^+ and Γ_C^-. In this case, the linear condition $\sigma_{22}(u) = 0$ of stress-free crack surfaces is not consistent, and it must be replaced with complementarity type conditions of non-penetration (Khludnev and Kovtunenko, 2000):

$$[\![u_2]\!] \geq 0,\ [\![\sigma_{22}(u)]\!] = 0,\ \sigma_{22}(u) \leq 0,\ \sigma_{22}(u)[\![u_2]\!] = 0 \quad \text{on } \Gamma_C \tag{66}$$

Similarly, if we invert the direction of loading g to $-g$ then $-u$ solves (64). Hence, the inter-penetration $[\![u_2]\!] < 0$ can occur even under mode-2 and mode-3 loading when $\beta \neq 0, \pm\pi/2$, in contrast to the plane isotropic/ orthotropic models. Again, one needs to use (66) to guarantee a non-penetration in this case, too.

Numerical realization of (66) with a generalized Newton method was suggested in Hintermüller et al. (2004). For the derivation of the shape derivative (39) under the non-penetration conditions (66) we refer to the works (Khludnev and Sokolowski, 1999; Khludnev and Kovtunenko, 2000; Kovtunenko, 2003).

4.2. Discretization of the problem

We discretize the problem by arguments of finite elements. For basis functions e^k defined in a k-th nodal point of the element, if we order the displacement vector as $\ldots, (u_1)^k, (u_2)^k, (u_3)^k, \ldots, (u_1)^s, (u_2)^s, (u_3)^s, \ldots$, then the stiffness matrix includes the following 3×3-cells:

$$\begin{bmatrix} C^\beta_{11} e^k_{,1} e^s_{,1} + C^\beta_{44} e^k_{,2} e^s_{,2} & C^\beta_{12} e^k_{,1} e^s_{,2} + C^\beta_{44} e^k_{,2} e^s_{,1} & C^\beta_{16} e^k_{,1} e^s_{,1} + C^\beta_{45} e^k_{,2} e^s_{,2} \\ C^\beta_{12} e^k_{,1} e^s_{,2} + C^\beta_{44} e^k_{,2} e^s_{,1} & C^\beta_{44} e^k_{,1} e^s_{,1} + C_{22} e^k_{,2} e^s_{,2} & C^\beta_{45} e^k_{,1} e^s_{,2} + C^\beta_{26} e^k_{,2} e^s_{,1} \\ C^\beta_{16} e^k_{,1} e^s_{,1} + C^\beta_{45} e^k_{,2} e^s_{,2} & C^\beta_{45} e^k_{,1} e^s_{,2} + C^\beta_{26} e^k_{,2} e^s_{,1} & C^\beta_{66} e^k_{,1} e^s_{,1} + C^\beta_{55} e^k_{,2} e^s_{,2} \end{bmatrix}$$

We suggest an adaptive meshing with the local refinement in a layer near the interface Σ including the crack Γ_C. In this construction we use two mesh-parameters: h for the uniform meshing in domain, and h_C for the fine meshing at interface, which are illustrated in Figure 3 for $h = 1/8$ and $h_C = h, h/2, h/4$.

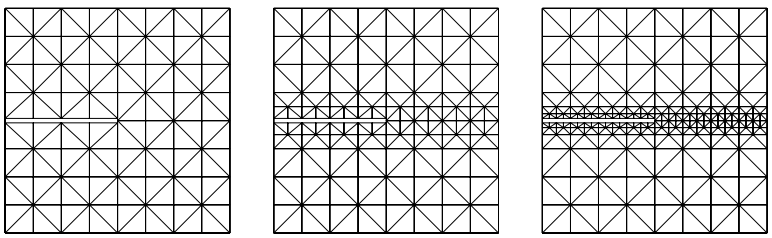

Fig. 3 Adaptive meshing in Ω_C for $h = 1/8$

To test the discretization error we exploit 3 singular solutions known for the plane isotropic model ($\beta = 0$):

$$U^1 = \frac{\sqrt{r}}{4\sqrt{2\pi}\,\mu}\left((2\varkappa - 1)\cos\frac{\phi}{2} - \cos\frac{3\phi}{2}, (2\varkappa + 1)\sin\frac{\phi}{2} - \sin\frac{3\phi}{2}, 0\right)^\top$$
$$U^2 = \frac{\sqrt{r}}{4\sqrt{2\pi}\,\mu}\left((2\varkappa + 3)\sin\frac{\phi}{2} + \sin\frac{3\phi}{2}, -(2\varkappa - 3)\cos\frac{\phi}{2} - \cos\frac{3\phi}{2}, 0\right)^\top \tag{67}$$
$$U^3 = \frac{\sqrt{2r}}{\sqrt{\pi}G_3}\left(0, 0, \sin\frac{\phi}{2}\right)^\top, \quad \varkappa = \frac{3\mu + \lambda}{\mu + \lambda}$$

given in polar coordinates $x_1 - l = r\cos\phi$, $x_2 - 0.5 = r\sin\phi$, which correspond to mode-1, mode-2, mode-3 crack, respectively. We take their sum:

$$u^{\text{singular}} = U^1 + U^2 + U^3 \tag{68}$$

as the exact solution to the Dirichlet-type problem:

$$\begin{aligned} &-\operatorname{div}\sigma(u) = 0 \quad \text{in } \Omega_C, \\ &\sigma_{12}(u) = \sigma_{22}(u) = \sigma_{23}(u) = 0 \quad \text{on } \Gamma_C^{\pm}, \\ &u = u^{\text{singular}} \quad \text{on } \Gamma_D \cup \Gamma_N \end{aligned} \tag{69}$$

First, we substitute the exact singular solution (68) into integrals in (36) and (41) with $f = g = 0$, calculate them numerically for $h = h_C = 1/20, 1/40, \ldots, 1/640$, and next we extrapolate obtained points at $h = 0$. In such manner the reference values are found for $l = 0.5$:

$$P(0.5) \approx 1.509 \times 10^{-4}(mPa \cdot m^2), \;\; P'(0.5) \approx -3.0425 \times 10^{-4}(mPa \cdot m) \tag{70}$$

Second, solving (69) numerically finds approximate values of the potential energy $P(l)$ and its shape derivative $P'(l)$ from (36) and (41) with $f = g = 0$. For numerical calculations the corresponding cut-off function χ in formula (41) is taken piecewise-linear in Ω with $\chi = 1$ around the crack tip, $\chi = 0$ by attaining the external boundary $\partial\Omega$, and it is centered with respect to each crack tip $(l, 0)$.

Computed values of P and P' were compared with the reference ones to evaluate an absolute error of the energy and its derivative by the discretization. For fixed $l = 0.5$ the result of calculations is depicted in Figure 4 for various mesh-size parameters h and h_C. This picture shows a linear convergence of both P and P' by the decreasing of h as well as h_C.

In further calculations we use $h = 1/80$ and $h_C = h/4 = 1/320$.

4.3. Crack under mode-1 loading

We consider the elastic problem (64) of Section 4.1 with a mode-1 loading:

$$g_2^{\pm} = \pm g_0, \quad g_1^{\pm} = g_3^{\pm} = 0, \quad g_0 = 0.001\mu \approx 3.5376(mPa) \tag{71}$$

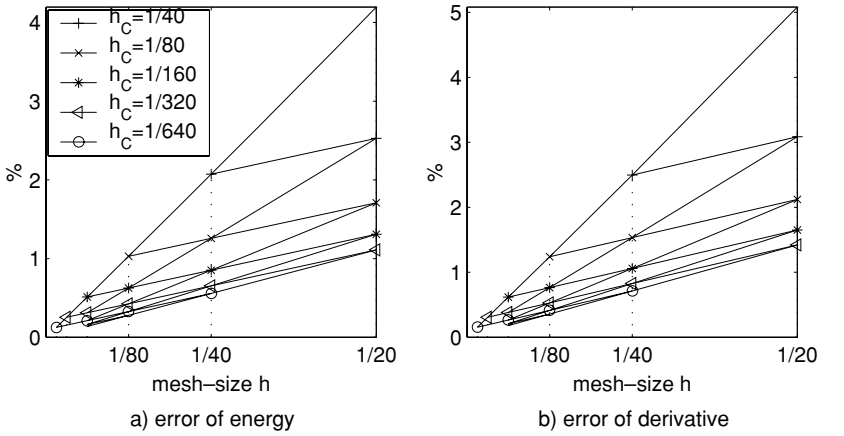

Fig. 4 Error by refinement of the mesh

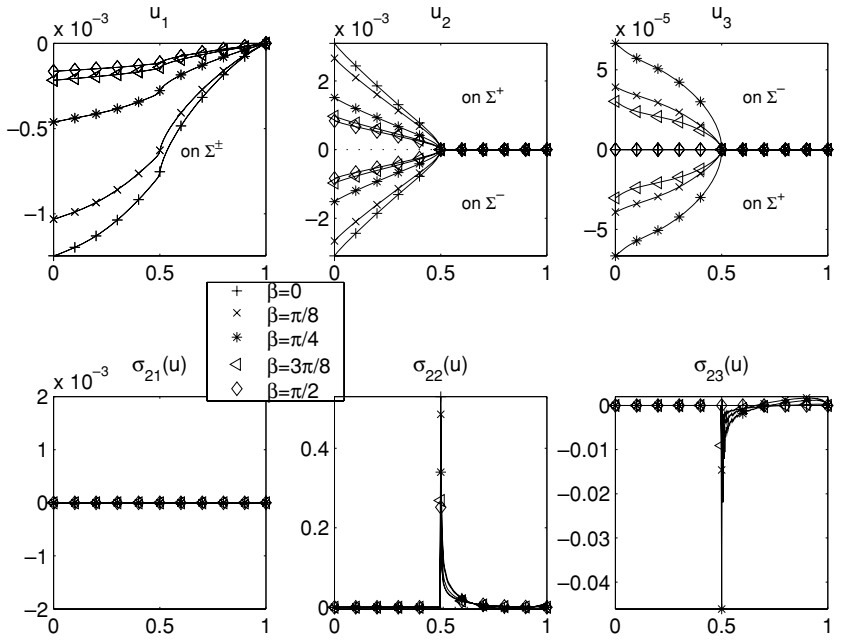

Fig. 5 Mode-1: Displacement and stress at interface

Its solution u defined in the variational form (33) is calculated numerically as described in Section 4.2.

For $l = 0.5$, the corresponding values of displacement u_1, u_2, u_3 and stress $\sigma_{12}(u)$, $\sigma_{22}(u)$, $\sigma_{23}(u)$ at the interface surfaces $\Sigma^{\pm}$ are depicted in Figure 5 in dependence of $\beta = 0, \pi/8, \pi/4, 3\pi/8, \pi/2$. Note that $\beta = \pi/4$ implies that fibers in Ω^+ and Ω^- are orthogonal. We can observe in Figure 5 clearly the appearance of a mixed mode-1 ($[\![u_2]\!] > 0$) together with mode-3 ($[\![u_3]\!] < 0$) crack under pure mode-1 loading for the spatial model in

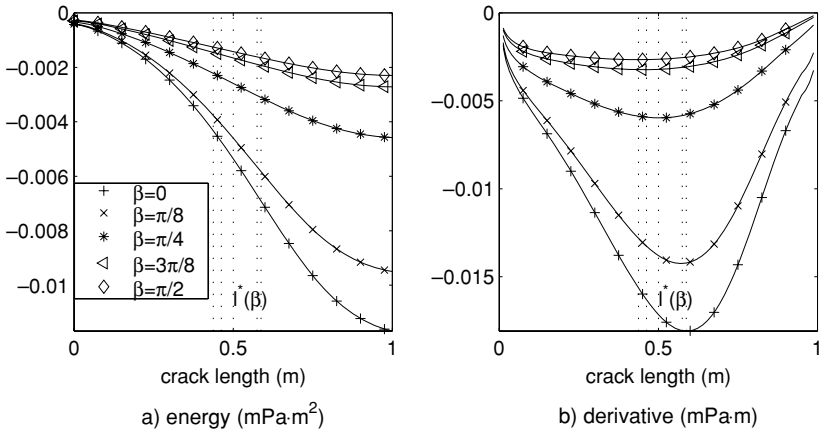

Fig. 6 Mode-1: Potential energy and its shape derivative

plane deformation, in contrast to the plane isotropic ($\beta = 0$) and orthotropic ($\beta = \pi/2$) models. The phenomenon of mode mixing come from the specialities of 3-dimensional elasticity model, which are particularly taken into account by the modelling.

Utilizing numerically formulas (36) and (41) with $f = 0$ as this was described in Section 4.2, we calculate the potential energy $P(l)$ and its shape derivative $P'(l)$ for discrete values of the length-parameter l. The crack tips are taken in nodal points $l = 0, h, \ldots, 1$ for P and $l = h, 2h, \ldots, 1 - h$ for P'. The definition of derivative in (38)–(39) does not allow us to consider the limit points $l = 0, 1$ in the latter case. The result of calculations is depicted in Figure 6 for $\beta = 0, \pi/8, \pi/4, 3\pi/8, \pi/2$.

We find the point(s) $l^\star \in (0, 1)$ of local extremum for $P'(l)$ where

$$P''(l^\star) = 0 \tag{72}$$

Henceforth, $P(l)$ is either convex or concave in intervals between $l = 0$, $l = l^\star$, and $l = 1$. For every β there happens only 1 point of local minimum $l^\star(\beta)$ where (72) is satisfied: $l^\star(0) \approx 0.5875$, $l^\star(\pi/8) \approx 0.575$, $l^\star(\pi/4) \approx 0.5$, $l^\star(3\pi/8) \approx 0.4625$, $l^\star(\pi/2) \approx 0.4375$, which are marked by dotted-lines in Figure 6.

4.4. Delamination under mode-1 loading

Now we proceed the consideration of Section 3.5 to describe a quasi-static process of delamination of the composite material with the interface crack via the shape optimization problem (53). For numerical tests we fix the physical value $\gamma = 25^2/2\mu \approx 0.011(mPa \cdot m)$ and use the numerical data of $P(l)$ and $P'(l)$ presented in Figure 6.

Let us scale the loading parameter $t \geq 0$ with g_0 and consider the linear loading $g_0 t(mPa)$. In view of the non-positiveness property of $P'(l)$ we calculate the function $G(t, l) = 0$ from (61) for $l \in (0, 1)$ and construct the corresponding curve in dependence of the loading $g_0 t$:

$$0 = g_0 G(t, l) = g_0 t - g_0 \sqrt{\gamma/(-P'(l))} \tag{73}$$

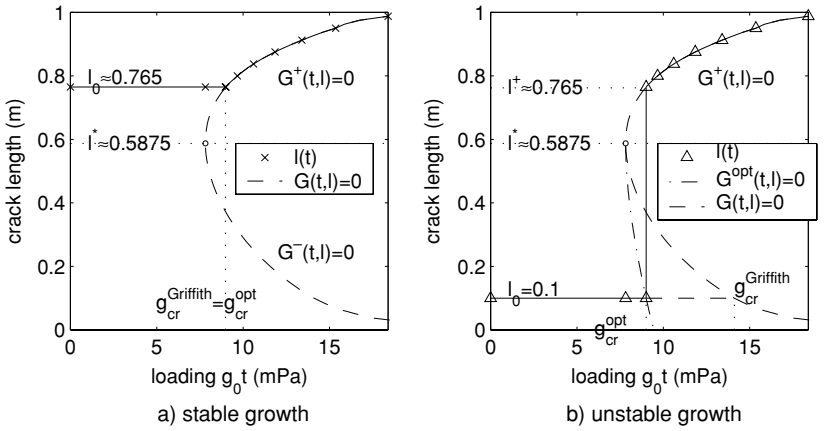

Fig. 7 Mode-1: Quasi-static crack growth as $\beta = 0$

which is depicted for $\beta = 0$ with a dashed-line in Figure 7. Let us fix arbitrary $l_0 \in (0, 1)$. Following the Griffith fracture hypothesis, the value of:

$$g_{cr}^{\text{Griffith}}(l_0) := g_0 t \quad \text{for } t : G(t, l_0) = 0 \tag{74}$$

implies the critical loading required to start the growth of an initial crack of the length l_0. In other words, the time-independent function $l(t) = l_0$ is a unique solution of (60) for $t : G(t, l_0) < 0$.

Let us look for a solution $l(t)$ to (60) for $t : G(t, l_0) \geq 0$. To do it, we find a point $l^\star \in (0, 1)$ such that

$$\frac{\partial G}{\partial l}(t, l^\star) = 0 \tag{75}$$

Note that (75) is independent on t. For $\beta = 0$ we get a unique $l^\star \approx 0.5875$, which is marked with a dotted-line in Figure 7. This point separates $G(t, l) = 0$ into two branches of an inverse-able function: $G^-(t, l) = 0$ for $l \in (0, l^\star)$, and $G^+(t, l) = 0$ for $l \in [l^\star, 1)$. For $t : G(t, l_0) \leq 0$ the local solution $l(t) = l_0$ of 60 meets either $G^-(t, l) = 0$ for $l_0 < l^\star$, or $G^+(t, l) = 0$ for $l_0 \geq l^\star$. The latter branch $G^+(t, l) = 0$ is an increasing function of l in $t : G^+(t, l) \geq 0$. Hence, if the initial crack is of the length $l_0 \in [l^\star, 1)$, then $l(t)$ satisfying $G^+(t, l(t)) = 0$ is a unique continuous solution to (60) for $t : G(t, l_0) \geq 0$. Conversely, $G^-(t, l) = 0$ is a decreasing function of l in $t : G^-(t, l) \geq 0$. Hence, for the initial crack of the length $l_0 \in (0, l^\star)$ there is no solution $l(t)$ to 60 which would be continuous at the point $t : G(t, l_0) = 0$. In (Kovtunenko, 2003) we suggested to extend the solution set to discontinuous solutions with a jump at $t : G(t, l_0) = 0$ by setting $l(t) : G^+(t, l(t)) = 0$.

To clarify the feature of the Griffith fracture law (60) we observe that it implies the local optimality criterion for minimization of the total potential energy with respect to shape parameter l of the crack length. Two Definitions (72) and (75) of $l^\star$ are equivalent due to $\partial G(t, l)/\partial l = 0.5\, P''(l)/P'(l)\sqrt{-P'(l)/\gamma}$. Thus, $P(l)$ is convex (and hence the total energy $\gamma l + t^2 P(l)$ is convex) if $\frac{\partial}{\partial l} G(t, l) < 0$ holds (the branch $G^+(t, l) = 0$). Respective $P(l)$ is concave if $\frac{\partial}{\partial l} G(t, l) > 0$ (the branch $G^-(t, l) = 0$). Henceforth, $G^+(t, l) = 0$ presents local

minima of the total potential energy with respect to l in $(l^\star, 1)$, but the local minima occur always at the boundary of an arbitrary minimization interval inside $(0, l^\star)$.

Now we look for a global minimizer to the shape optimization problem (53) presented in the form (62), (63). Solving it numerically we find continuous solutions for initial cracks of the length $l_0 \in [l^\star, 1)$, which are here the same as obtained before by the Griffith fracture law (60). For $\beta = 0$ and $l_0 \approx 0.765$ the solution $l(t)$ to (62), (63) is depicted with a solid line in Figure 7 (a) and marked as "stable growth". For initial cracks of the length $l_0 \in (0, l^\star)$ we derive discontinuous solutions with a jump $l^+ - l_0 > 0$ at the point t where (59) is attained:

$$g_{\rm cr}^{\rm opt}(l_0) := g_0 t \quad \text{for } t : G(t, l^+) = 0,\ \gamma[l^+ - l_0] + t^2[P(l^+) - P(l_0)] = 0 \tag{76}$$

For $\beta = 0$ and $l_0 = 0.1$ the solution $l(t)$ to (62), (63) is depicted with a solid line in Figure 7 (b) and marked as "unstable growth" . We computed $l^+ \approx 0.765$ (exactly this value was taken before for l_0 in the previous example on stable propagation), $g_{cr}^{\rm opt} \approx 9(mPa)$ and $g_{\rm cr}^{\rm Griffith} \approx 14(mPa)$. Here the value of critical loading obtained by the shape optimization approach (76) is less than one predicted by the Griffith fracture criterion (74).

Solving numerically the shape optimization problem (62), (63) as described before for all discrete values of the initial crack length $l_0 \in (0, l^\star)$ from (76) we improve the curve of critical loading:

$$0 = G^{\rm opt}(t, l) := \begin{cases} G^+(t, l) & \text{for } l \in [l^\star, 1) \\ g_0 t - g_{\rm cr}^{\rm opt}(l) & \text{for } l \in (0, l^\star) \end{cases} \tag{77}$$

For $\beta = 0$ this curve is depicted with a dash-dot line in Figure 7 b). Consequently, a delamination of the initial crack of length $l_0 \in (0, 1)$ under the linear quasi-static loading $g_0 t$ can be described geometrically by the following algorithm.

Algorithm 1.

(0) *Fix an initial crack length* $l_0 \in (0, 1)$*;*
(1) no growth: $l(t) = l_0$ *for* $t : G^{\rm opt}(t, l_0) < 0$*;*
(2) initiation: $l(t) = \max\{l_0, l^+\}$ *such that* $G^{\rm opt}(t, l^+) = 0$ *at* $t : G^{\rm opt}(t, l_0) = 0$*;*
(3) growth: $l(t) = l$ *such that* $G^+(t, l) = 0$ *for* $t : G^{\rm opt}(t, l_0) > 0$*.*

If $l^+ = l_0$ in Step 2 then the propagating crack is stable and it grows in a continuous way, else $l^+ > l_0$ then the crack propagation is unstable with the jump $l^+ - l_0$.

Next we calculate the curves of $G^{\rm opt}(t, l) = 0$ (optimization approach) for various parameters of $\beta = 0, \pi/8, \pi/4, 3\pi/8, \pi/2$, which are depicted in Figure 8. For comparison, $G(t, l) = 0$ (the Griffith criterion) are drawn with a dashed line. There are found the values of $l^\star(\beta)$ from (75) separating the cases of stable and unstable crack crack propagation and indicated with dotted lines in the picture. For every initial crack of length l_0 the delamination process can be described by Algorithm 1.

Note that Figure 8 shows clearly theoretical intention $g_{\rm cr}^{\rm Griffith}(l_0) \to \infty$ as $l_0 \to 0$. The limit case $l_0 = 0$ means a birth of the crack in a continuous solid. The physic of this phenomenon involves micro-cracks and hence can not be described correctly by the above macro-crack modelling. Nevertheless, from Figure 8 we observe a finite limit of $g_{\rm cr}^{\rm opt}(0) < \infty$, which seems to be more consistent physically than $g_{\rm cr}^{\rm Griffith}(0) = \infty$.

The other limit behavior $g_{\rm cr}^{\rm opt}(l_0) = g_{\rm cr}^{\rm Griffith}(l_0) \to \infty$ as $l_0 \to 1$ is here due to the boundary condition of clamping edge as $l = 1$. For the relaxed boundary condition: $u_1 = 0$, $\sigma_{12}(u) =$

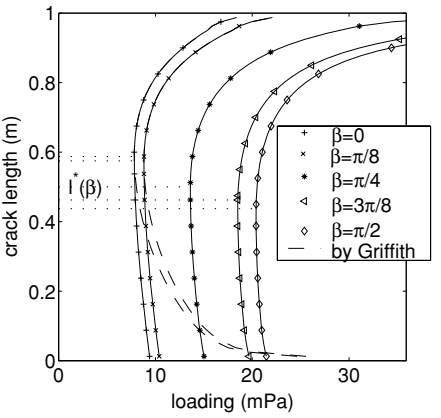

Fig. 8 Mode-1: Curves $G^{\mathrm{opt}}(t,l)=0$ of critical loading

$\sigma_{13}(u)=0$ at Γ_D we obtained in Kovtunenko (2004) that $g_{\mathrm{cr}}^{\mathrm{Griffith}}(l_0)\to 0$ as $l_0\to 1$ ($\beta=0$) implying a break of the composite material along the interface.

4.5. Interface crack and delamination under mode-2 loading

For the same geometric and physical data of Section 4.1 we apply the following mode-2 loading to problem (64):

$$g_1^{\pm}=\pm g_0,\quad g_2^{\pm}=g_3^{\pm}=0,\quad g_0=0.001\mu\approx 3.5376\,(mPa) \tag{78}$$

illustrated in Figure 2. Its numerical solution u is found from the variational formulation given in Section 3.2 utilizing the discretization of Section 4.2. In Figure 9 the corresponding displacement and stress are depicted at the interface including the crack Γ_C of fixed length $l=0.5$ for various parameters $\beta=0,\pi/8,\pi/4,3\pi/8,\pi/2$. From this picture we point out a coupling between components (u_1,u_2) and u_3 of the displacement in the spatial model suggested. For all cases of β we have here pure mode-2 crack.

Using formulas (36) and (41) with $f=0$ of Section 3.3, next we calculate the potential energy $P(l)$ and its shape derivative $P'(l)$ for the discrete parameter l of the crack tip located in nodal points of the mesh. The results are presented in Figure 10 together with points $l^\star(\beta)$ computed from (72) as $l^\star(0)\approx 0.325$, $l^\star(\pi/8)\approx 0.3375$, $l^\star(\pi/4)=l^\star(3\pi/8)\approx 0.35$, $l^\star(\pi/2)\approx 0.3625$.

Utilizing the problem of shape optimization with data shown in Figure 10 as described in Section 4.4, for mode-2 loading we derive similarly the curves of critical loading: $G^{\mathrm{opt}}(t,l)=0$ (optimization) and $G(t,l)=0$ (the Griffith fracture law), which are depicted in dependence of g_0t in Figure 11.

4.6. Interface crack and delamination under mode-3 loading

Finally, we apply the mode-3 loading to problem (64):

$$g_3^{\pm}=\pm g_0,\quad g_1^{\pm}=g_2^{\pm}=0,\quad g_0=0.001\,\mu\approx 3.5376\,(mPa) \tag{79}$$

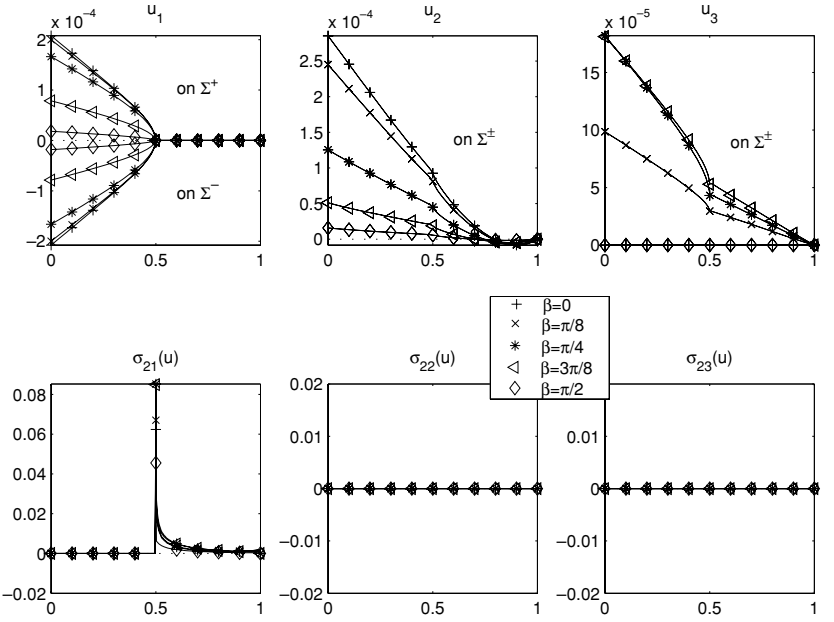

Fig. 9 Mode-2: Displacement and stress at interface

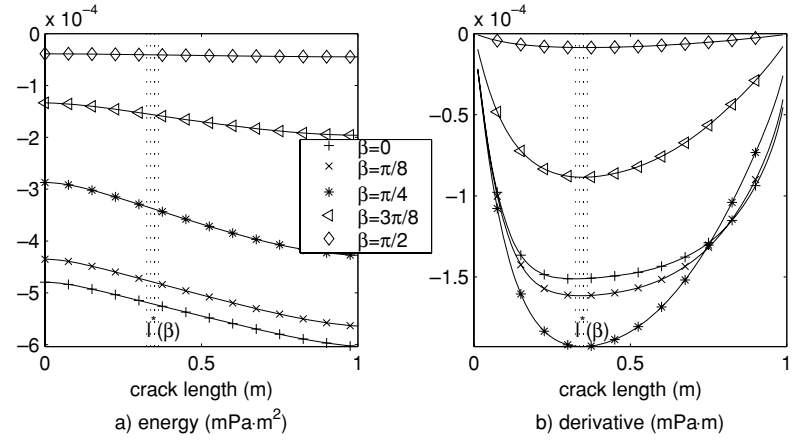

Fig. 10 Mode-2: Potential energy and its shape derivative

An additional state of the system is calculated as $\beta = \pi/16$ to see a non-monotone behavior at $\beta = \pi/8$ later. From Figure 12 presenting the displacement and stress at the interface with the crack Γ_C of length $l = 0.5$ we conclude that the crack appears in a mixed mode-1 with mode-3 state under pure mode-3 loading for $\beta \neq 0, \pi/2$. Let us also note that inverting β to $-\beta$ gets here the negative jump $[\![u_2]\!] < 0$ at Γ_C, which implies an inter-penetration of the cracks surfaces. This fact would be physically inadmissible and required the using of non-penetration conditions, as this was discussed at the end of Section 4.1.

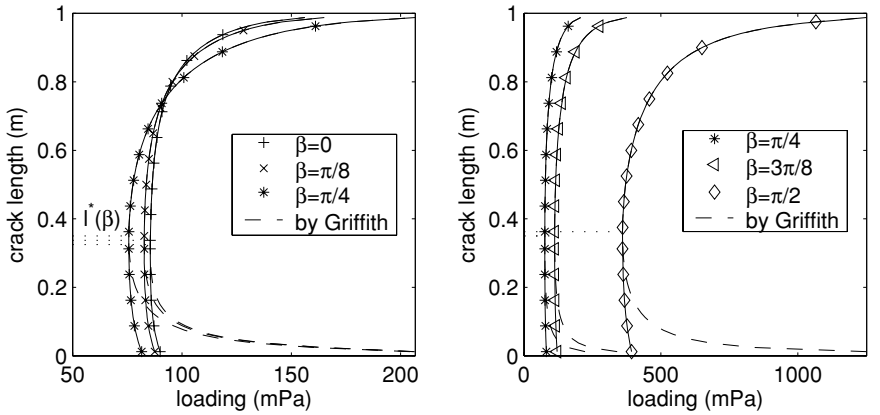

Fig. 11 Mode-2: Curves $G^{\text{opt}}(t, l) = 0$ of critical loading

In Figure 13 there are depicted the corresponding potential energy $P(l)$ and its shape derivative $P'(l)$ together with $l^\star(0) = l^\star(\pi/2) \approx 0.3$ and $l^\star(\pi/16) = l^\star(\pi/8) = l^\star(\pi/4) = l^\star(3\pi/8) \approx 0.2875$. In the picture we observe the non-monotone behavior with respect to β near $\beta = \pi/8$.

The curves of $G^{\text{opt}}(t, l) = 0$ and $G(t, l) = 0$ for the quasi-static delamination under mode-3 loading are presented in Figure 14.

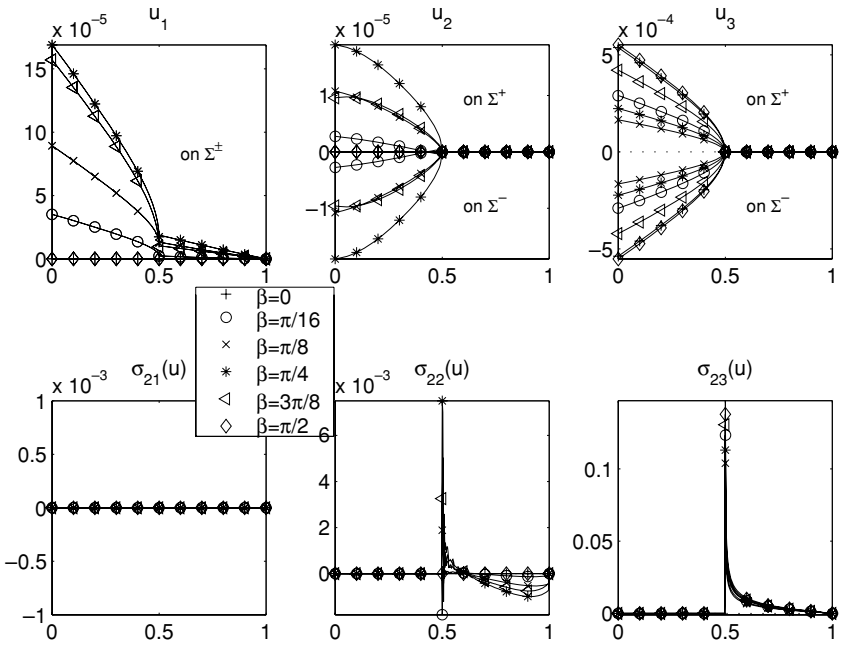

Fig. 12 Mode-3: Displacement and stress at interface

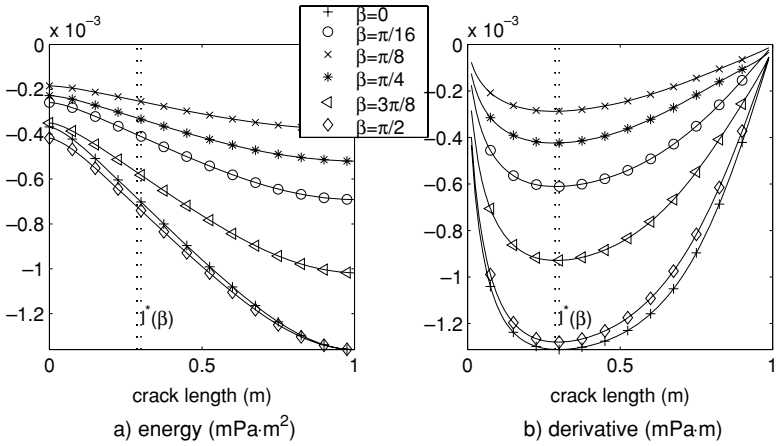

Fig. 13 Mode-3: Potential energy and its shape derivative

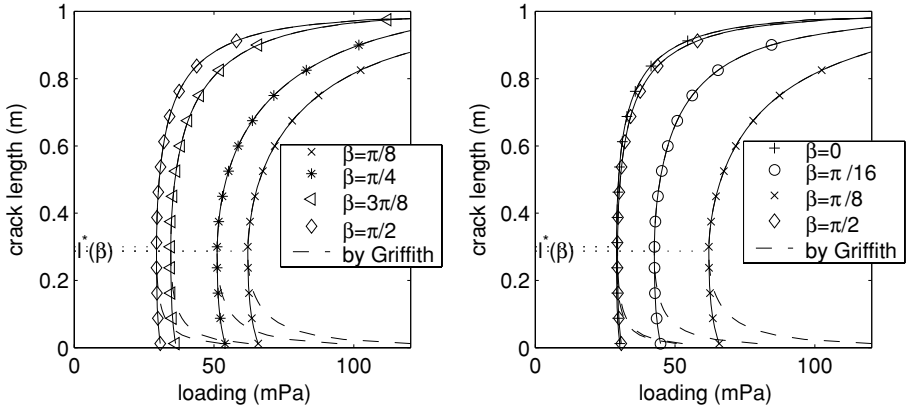

Fig. 14 Mode-3: Curves $G^{\text{opt}}(t, l) = 0$ of critical loading

5. Conclusion

As the principal findings we stress on the following features of the spatial model for an interface crack in a composite material:

- Under pure mode-1 as well as mode-3 loading the interface crack appeared always in the mixed mode-1 with mode-3 state for $\beta \neq 0, \pm\pi/2$, that indicates a spatial character of the 2.5-dimensional model suggested;
- Under pure mode-3 loading an inter-penetration between opposite crack surfaces can occur, therefore, the stress-free boundary condition should be replaced with non-penetration conditions at the crack;
- If a stable path of the crack propagation is not reachable, then the critical loading needed to initiate a delamination of the composite was found from the global shape optimization problem, and it was obtained smaller than one required by the Griffith fracture law.

Acknowledgment The research results were obtained with support of the Austrian Science Fund (FWF) in framework of the SFB project F003 "Optimierung und Kontrolle" and the Lise Meitner project M622/ M737 "Variational methods in application to crack problems", and the INTAS project 03-51-6046.

The author is thankful to Dr. I.I. Argatov from St.-Petersburg for the discussion and useful remarks on the modelling.

References

Argatov II, Bach M, Kovtunenko VA (2003) Propagation of the mode-1 crack under Irwin and Khristianovich-Barenblatt criterions. Phys-Chemical Mech Materials 55–58

Bach M, Nazarov SA, Wendland WL (2000) Stable propagation of a mode-1 planar crack in an anisotropic elastic space. Comparison of the Irwin and the Griffith approaches. Current Problems Anal. Math. Phys. (Taormina, 1998) 167–189, Aracne, Rome

Bourdin B, Francfort GA, Marigo JJ (2000) Numerical experiments in revisited brittle fracture. J. Mech. Phys. Solids 48:797–826

Cherepanov EG (1979) Mechanics of brittle fracture McGrow-Hill

Dal Maso G, Toader R (2002) A model for the quasistatic growth of brittle fractures: existence and approximation results. Arch Rational Mech Anal 162:101–135

Francfort GA, Marigo JJ (1998) Revisiting brittle fracture as an energy minimization problem. J Mech Phys Solids 46:1319–1342

Friedman A, Hu B, Velazquez JJL (2000) The evaluation of stress intensity factors and the propagation of cracks in elastic media. Arch Rat Mech Anal 152:103–139

Friedman A, Liu Y (1996) Propagation of cracks in elastic media. Arch Rat Mech Anal 136:235–290

Guddat J, Nowack D (1991) Parametric optimization: pathfollowing and jumps in the set of local minimizers and in the critical set. In: Guddat J, Jongen H Th, Kummer B, Nožička F (eds.), Parametric Optimization and Related Topics II, Akademie Verlag, Berlin pp. 76–111

Hintermüller M, Kovtunenko VA, Kunisch K (2004) The primal-dual active set method for a crack problem with non-penetration. IMA J Appl Math 69:1–26

Jongen H Th, Stein O (1997) Parametric semi-infinite programming: jumps in the set of local minimizers. In: Guddat J, Jongen H-Th, Nožička F, Still G, Twilt F (eds.), Parametric Optimization and Related Topics IV, Peter Lang, Frankfurt am Main, pp. 161–176

Khludnev AM, Kovtunenko VA (2000) Analysis of cracks in solids WIT-Press, Southampton. Boston

Khludnev AM, Sokolowski J (1999) The Griffith formula and the Cherepanov-Rice integral for crack problems with unilateral conditions in nonsmooth domains. Euro J Appl Math 10:379–394

König M, Krüger R, Kussmaul K, von Alberti M, Gädke M (1997) Characterizing static and fatigue interlaminar fracture behavior of a first generation graphite/epoxy composite. In: Hooper JS (ed.), 13th Composite Materials: testing and design ASTM STP 1242 ASTM, Vol. 13, pp. 60–81

Kovtunenko VA (2003) Invariant energy integrals for the non-linear crack problem with possible contact of the crack surfaces. J Appl Maths Mechs 67:99–110

Kovtunenko VA (2003) Quasistatic propagation of cracks. In: Wendland WL and Efendiev M (eds.), analysis and simulation of multifield problems, Lecture Notes Appl Comp Mech 12:227–232, Springer, 2003

Kovtunenko VA (2004) Numerical simulation of the non-linear crack problem with non-penetration. Math Meth Appl Sci 27:163–179

Kovtunenko VA (2005) Nonconvex problem for crack with nonpenetration. Z Angew Math Mech 85:242–251

Leblond JB (1999) Crack paths in three-dimensional elastic solids. I. Two-term expansion of the stress intensity factors—application to crack path stability in hydraulic fracturing. Int J Solids Structures 36:79–103

Lekhnitskii SG (1963) Theory of elasticity of an anisotropic body, Holden-Day, San Francisco

Mielke A, Theil F, Levitas VI (2002) A variational formulation of rate-independent phase transformations using an extremum principle. Arch Rational Mech Anal 162:137–177

Morozov NF (1984) Mathematical foundation of the crack theory, Nauka, Moscow, in Russian

Nazarov SA (1998) The interface crack in anisotropic bodies: Stress singularities and invariant integrals. J Appl Maths Mechs 62:453–464

Ni L, Nemat-Nasser S (1991) Interface cracks in anisotropic dissimilar materials: An analytic solution. J Mech Phys Solids 39:113–144

Rice JR (1978) Thermodynamics of the quasi-static growth of Griffith cracks. J Mech Phys Solids 26:61–78

Rochde A, Stavroulakis GE (1997) Genericity results for path-following in discretized unilateral contact mechanics. In: Jongen H-Th, Nožička F, Still G, Twilt F, (eds.), Parametric Optimization and Related Topics J. Guddat, Peter Lang, Frankfurt am Main, 4:315–328

Suo Zh (1990) Singularities, interfaces and cracks in dissimilar anisotropic media. Proc R Soc Lond A 427:331–358

Ting TCT (1986) Explicit solution and invariance of the singularities at an interface crack in anisotropic composites. Int J Solids Structures 22:965–983